Drone CO_2 Measurements During the Tajogaite Volcanic Eruption

John Ericksen[1], Tobias P. Fischer[2], G. Matthew Fricke[1], Scott Nowicki[2], Nemesio M. Pérez[3], Pedro Hernández Pérez[3], Eleazar Padrón González[3], and Melanie E. Moses[1,4]

[1]Computer Science Department, University of New Mexico, Albuquerque, New Mexico, USA
[2]Department of Earth and Planetary Sciences, University of New Mexico, Albuquerque, New Mexico, USA
[3]Instituto Volcanológico de Canarias (INVOLCAN), Tenerife, Islas Canarias, Spain
[4]Santa Fe Institute, Santa Fe, New Mexico, USA

Correspondence: Tobias P. Fischer (fischer@unm.edu), G. Matthew Fricke (mfricke@unm.edu)

Abstract. We report in-plume carbon dioxide (CO_2) concentrations and carbon isotope ratios during the 2021 eruption of Tajogaite Volcano, La Palma Island, Spain. CO_2 measurements inform our understanding of volcanic contributions to the global climate carbon cycle and the role of CO_2 in eruptions. Traditional ground-based methods of CO_2 collection are difficult and dangerous and as a result only about 5% of volcanoes have been directly surveyed. We demonstrate that UAS surveys allow for fast and relatively safe measurements. Using CO_2 concentration profiles we estimate the total flux during several measurements in November 2021 to be $4.59 \pm 0.46 \times 10^3$ to $2.85 \pm 0.28 \times 10^4 \, \mathrm{t\,day^{-1}}$. Carbon isotope ratios of plume CO_2 indicate a deep magmatic source, consistent with the intensity of the eruption. Our work demonstrates the feasibility of UAS for CO_2 surveys during active volcanic eruptions, particularly for deriving rapid emission estimates.

1 Introduction

Measurements of volcanic CO_2 emissions during eruptions are critical for understanding magma and eruption dynamics. CO_2 is a significant greenhouse gas (Arrhenius, 1896) and making measurement of CO_2 emissions is important for climate science. CO_2 gas is second only to water vapor in abundance in volcanic emissions (Giggenbach, 1996). Despite the significance and abundance of CO_2 in the Earth System in general and in magmatic systems in particular, measuring the emission rates of this gas from volcanic craters, diffuse sources, and low-level hydrothermal sites has remained a major challenge (Fischer and Aiuppa, 2020). As a result, detailed CO_2 surveys have been conducted at just 5% of volcanoes (Fischer et al., 2019).

The main contributions of this work are that, for the first time, we estimate CO_2 flux using direct in-plume CO_2 measurements rather than using in-plume CO_2 to SO_2 ratios combined with separately measured SO_2 emissions. The second major contribution is that we perform in-situ gas sample-return during a major volcanic eruption for carbon isotope measurements. We use the Dragonfly Unpiloted Aerial System (UAS) (Ericksen et al., 2022) to gather samples directly from the eruption plume (Figure 1). The UAS transects the plume and employs an onboard infrared (IR) sensor to continuously obtain concentration readings. These readings are then used to estimate a 2D isotropic Gaussian concentration model. In-plume wind speed measurements in combination with the plume model allow us to estimate CO_2 flux. While our technique has similarities to the 'ladder traverse' technique utilizing large in-situ sensing equipment mounted on a piloted fixed-wing aircraft (Werner et al.,

Figure 1. A Dragonfly UAS returning from a CO₂ sample mission during the November 2021 eruption of Tajogaite volcano. The large volcanic ash plume is visible in the background and contains an invisible CO_2 plume, which was the mapping target of this drone.

2013), it has the obvious advantages of being much less costly, logistically less challenging, and less hazardous. Since our approach extrapolates the shape of the plume it requires far fewer plume transects. Crucially, the Dragonfly UAS does not use a combustion engine, which previous work has shown to contaminate CO_2 measurements and samples with jet-fuel derived organic carbon (Fischer and Lopez, 2016). The resulting plume CO_2 concentration profile is used to guide the UAS to a productive sample return location of maximum concentration. Carbon isotope analyses of the samples reveal information, such as CO_2 source, which is relevant to predicting the course of the eruption. We tested this technique during the 2021 Tajogaite volcanic eruption on La Palma Island, Spain, and compared the resulting flux estimates to the traditional ground-based CO_2 to SO_2 ratio method. As we demonstrate, UASs provide a method for obtaining in-plume gas samples, concentrations, and wind velocity measurements. Together these data allow isotope ratios to be determined and estimation of CO_2 flux, furthering our understanding of volcano dynamics during an eruption and allowing predictions of eruption intensity and duration. Our technique can be widely used at passively degassing and erupting volcanoes to obtain near-real-time CO_2 flux measurements to better constrain the global volcanic CO_2 budget, and assess volcanic activity.

1.1 Related Work

While global initiatives to directly determine CO_2 flux from biogenic sources, i.e. FLUXNET (Office of Science, US DOE, 2023) have advanced our understanding of the surface carbon cycle, estimates of volcanic flux are to a large extent obtained by combining SO_2 flux measurements with observed CO_2 to SO_2 ratios (Fischer and Aiuppa, 2020). This approach relies on two separate sets of measurements utilizing a ground-based or space-based remote sensing technique to determine the SO_2 concentration of the volcanic plume and a direct sampling or sensing technique to determine the CO_2 to SO_2 ratio. In almost all cases, these two separate sets of measurements are not made simultaneously and result in intrinsic uncertainties in CO_2 flux estimates (Burton et al., 2013). CO_2 surveys have been performed using satellite-based approaches, for example, Johnson et al.

(2020) performed CO_2 flux estimates of the 2018 Kilauea Volcano. Their work utilized the Orbiting Carbon Observatory -2

45   (OCO-2) to measure the CO_2 emissions from the 2018 Klīlauea eruption. A measurement of 77.1±41.6 kt/day was obtained
during the one day of observations where conditions enabled the collection of consistent high-quality data. Cloud coverage and
aerosol are the major inhibitors for obtaining consistent CO_2 data using OCO-2. In addition, the wind direction must be near
perpendicular to the satellite's orbit path and the measurements must be made down-wind from the plume. The OCO-2 16-day
repeat cycle currently makes this method impractical for frequent, high-rate CO_2 flux measurements from erupting volcanoes

50   and the only other successful volcanic CO_2 emission study was by Schwandner et al. (2017) of Yasur in Vanuatu. Therefore,
space-based CO_2 instruments require favorable atmospheric conditions and satellite positioning and are not yet feasible for
volcano monitoring (Schwandner et al., 2017).

The value of UAS surveys of volcanic emissions was recognized by Xi et al. (2016) who surveyed passive degassing SO_2 at
Turrialba volcano, Costa Rica and estimated SO_2 flux. Other investigators have used UAS to measure plume SO_2 and collect

55   plume trace gases (Rüdiger et al., 2018) or use miniDOAS systems mounted on UAV to obtain SO_2 fluxes (Stix et al., 2018).
Recently UAS have been used to collect gas samples and measure gas compositions volcanic plumes from passively degassing
volcanoes in remote regions (Liu et al., 2020; Galle et al., 2021).

Gerlach et al. (1997) and Werner et al. (2013) estimate plume CO_2 flux using the parsimonious assumption that plumes are
uniform. They use the mean value to estimate the flux whereas we use our observations in the field that support the hypothesis

60   that plumes can be well modeled by Gaussian distributions. Our work relies on the assumption that a Gaussian model of the
plume cross-section results in more accurate estimates of total flux.

Burton et al. (2023) surveyed emissions of the Tajogaite eruption in early October 2021. Their survey included SO_2 measure-
ments by UAV that were used to infer CO_2 concentrations. Our work in late November complements the Burton et. al. survey
by providing additional information on the evolution of the eruption and by using a different CO_2 flux estimation method that

65   employs direct CO_2 measurements rather than CO_2/SO_2 ratios. Our estimates of CO_2 flux taken a month later were lower
than those of Burton et. al.

1.2 Background

La Palma Island is in Spain's Canary archipelago (Schmincke, 1982). The northern sector of the island hosts the oldest subaerial
(on land) volcanism, characterized by repeated large lateral edifice collapses (Day et al., 1999; Acocella et al., 2015). Volcanism

70   resulted in the formation of Garafía and Taburiente and then moved southward to form Cumbre Vieja volcano, at the southern
part of the island. This southern system represents the last stage in the geological evolution of La Palma island, as volcanic
activity has taken place exclusively on that part of the island for the last 123 ka (Carracedo et al., 1998). The most recent
volcanic eruption of Cumbre Vieja is Tajogaite (2021) (Carracedo et al., 2001; Ward and Day, 2001), preceded by that of
Teneguía in 1971 (Fernández et al., 2021) and San Juan in 1940 (Fernández et al., 2021; Albert et al., 2016). At 14:10 UTC on

75   September 19, 2021 Tajogaite volcano erupted from a vent on the western side of La Palma Island, in the vicinity of the Llano
del Banco eruptive center of the San Juan eruption of 1949 (Instituto Geográfico Nacional, 2022). The eruption was forecast
using seismic, geodetic and geochemical techniques by Spanish researchers who alerted the civil protection officials several

days before the start of the eruption (De Luca et al., 2022). The monitoring network of diffuse CO_2 emissions on La Palma detected magmatic CO_2 several months before the eruption (León et al., 2022; Rodríguez-Pérez et al., 2022). This monitoring activity took advantage of extensive previous work characterizing diffuse CO_2 emissions on La Palma. This work provided key insights into the dynamics of magmatic CO_2 degassing on the island (Padrón et al., 2015). The eruption itself began with an explosive phase that ejected ash to an altitude of 5 km, then transitioned to fire fountains, violent strombolian activity, and the production of highly fluid lava flows. Within 24 hours of the initial eruption a 3 km long lava flow was evident (Instituto Geográfico Nacional, 2022). The eruption lasted for more than 85 days and built a pyroclastic cone of about 225 m in height. Over the period of the eruption, the volcano showed dynamic and changing activity with new vents frequently opening on the active cone. These vents produced explosive and effusive eruptions of varying intensity (Castro and Feisel, 2022). Bulk tephra, matrix glass and glass inclusions have a basanitic-tephritic composition of 43 to 46 wt%.

Since the onset of the 2021 Tajogaite eruption on September 19, frequent measurements of SO_2 emission rates using miniDOAS traverses by car, ship, and helicopter were performed. Using this data a flux of over 5×10^4 t day^{-1} of SO_2 was estimated (Pérez et al., 2022). Daily monitoring of SO_2 gas emissions occurred before and throughout the eruption using TROPOMI data from the Sentinel 5P satellite (Copernicus SO_2 satellite monitoring, Smithsonian Institution's Global Volcanism Program 2021). The range of measured emissions rates depended upon wind direction and velocity, as well as eruptive style and activity. The measured SO_2 flux ranged from 3×10^4 to 5×10^4 t day^{-1} at the beginning of the eruption and a mean of 10^4 t day^{-1} over the duration of the active eruption (Albertos et al., 2022). These SO_2 emission rates are likely different from CO_2, but provide the best available proxy for CO_2 emissions and are a useful point of comparison for our UAS-based flux estimates in addition to the measurements made by Burton et al. 2023 in October 2021 which range from 3.36×10^4 to 4.19×10^4 t day^{-1}.

Additional gas monitoring techniques deployed during the eruption included stationary Multi-GAS and FTIR-based plume gas composition measurements as well as carbon isotope analyses of plume CO_2 in collaboration with the international volcanic gas community (Pérez et al., 2022).

2   Methods

Our aim was to measure plume CO_2 concentrations, calculate the resulting flux, and obtain isotope data from samples taken within the plume. To achieve these goals we utilized the Dragonfly UAS, with an approximate battery life of 50 min. This extended flight time enables long-distance transects to capture large plumes. CO_2 concentrations were measured by PP Systems SBA-5 IR sensor mounted on the Dragonfly with data transmitted to the pilot in real-time (Ericksen et al., 2022). Wind speeds were derived from the ERA5 model of the European Centre for Medium-Range Weather Forecasts 10 m height wind speeds corresponding to the time of each flight (Liu et al., 2020). These measurements were independently validated using a hand-held anemometer and the UAS drift method (Liu et al., 2020; Galle et al., 2021). For the drift method, a Dragonfly was programmed to maintain its altitude but not its lateral position and allowed to drift with the plume. We used this estimate of wind velocity within the plume with the highest CO_2 concentration (Plume B) to parameterize the flux estimation (Figure 2).

At the location with the highest measured CO_2 concentration, a timed trigger activated a small pump, and a plume gas sample was collected into a Tedlar bag (Figures 2 and 3). We also collected gas samples of the plume from the ground when the wind direction was favorable and volcanic activity permitted. Ground-based plume samples were analyzed by Infrared Isotope Spectroscopy with a Delta Ray located at the INVOLCAN Volcano Observatory, La Palma, following the procedure described previously (Fischer and Lopez, 2016; Ilanko et al., 2019). The error bounds on the $\delta^{13}C$ measurements are less than 0.1‰ for all analyses.

We also placed a Multi-GAS instrument at an accessible and safe location about 1 km to the north of the crater. Data from this instrument recorded CO_2 and SO_2 concentrations in the gas plume. The ratios were calculated using the Ratiocalc software and we report averages for each day of the experiment.

Crosswind transects were flown downwind of the eruption to encounter the plume. CO_2 was measured at 10 hz during flights across the plume at specified altitudes relative to launch. Each measurement was correlated to the latitude, longitude, altitude, and time of the UAS during flight, giving a CO_2 concentration cross-section of the plume.

We set the ambient background CO_2 to the value observed outside the plume for each flight. The actual measurements of ambient CO_2 were made well outside of the plume (up to 400 m away from the edge of the plume) and only vary from 415 to 430 ppm.

To estimate the total flux of the plume, we perform the following procedure.

1. Convert GPS coordinates into a linear distance from the launch point.

2. Isolate the plume by setting an ambient CO_2 threshold and removing data points less than that threshold.

3. Fit a Gaussian curve to the data set as follows.

    (a) Calculate the mean, μ, and standard deviation, σ, of the CO_2 across the transect.

    (b) Scale the two-dimensional Gaussian curve to fit the data by choosing a constant amplitude, a, using gradient descent to minimize the χ^2 difference between the model and plume sample data. We assume that the Gaussian shape is uniform in both x and y dimensions.

$$\text{GaussianModel2D}() = a\frac{e^{-\frac{1}{2}(\frac{x-\mu_x}{\sigma_x})^2}}{\sigma_x\sqrt{2\pi}}\frac{e^{-\frac{1}{2}(\frac{y-\mu_y}{\sigma_y})^2}}{\sigma_y\sqrt{2\pi}}$$

$$= a\frac{e^{-\frac{1}{2}(\frac{x-\mu}{\sigma})^2}}{\sigma\sqrt{2\pi}}\frac{e^{-\frac{1}{2}(\frac{0}{\sigma})^2}}{\sigma\sqrt{2\pi}} \qquad y=0, \mu_y=0, \sigma=\sigma_x, \sigma_y=\sigma, \mu=\mu_x$$

$$= a\frac{e^{-\frac{1}{2}(\frac{x-\mu}{\sigma})^2}}{\sigma^2 2\pi}$$

4. Integrate the two-dimensional Gaussian and multiply by the measured wind speed, v, to obtain plume flux in $\text{mgS}^{-1}\text{m}^{-2}$. Multiplying this again by the number of seconds in a day, and the number of mg in a ton gives the flux in $t\,day^{-1}$.

$$\int \text{GaussianModel2D}() = a\int \frac{e^{-\frac{1}{2}(\frac{x-\mu}{\sigma})^2}}{\sigma^2 2\pi} = a$$

$$\text{flux}(a,v) = v\,a$$

3 Results

Flux estimates are derived from the 3 UAS transects that crossed plume A. These transects were collected on November 26th and 27th, 2021. Other transects shown in Figure 2 either did not intersect any plume or did not cross the entire plume. In the latter case this resulted in a poor fit to the Gaussian distribution, violating our assumption of normality. We also report carbon isotopes of plume CO_2, and flux estimates based on the Multi-GAS CO_2/SO_2 ratios.

Table 1. CO_2 data collected by UAS across plumes A and B during the Tajogaite eruption. * Indicates transect with samples collected into Tedlar bags and analyzed by Infrared Isotope Ratio Spectroscopy. † Indicates transects that encountered plume B, but the gas distribution did not meet our Gaussian fit assumptions, as indicated by the large χ^2 value in comparison to the Gaussian amplitude.

Date	Transect	Altitude	Wind [$\mathrm{m\,s^{-1}}$]	Max Con. [ppm]	Gaussian Fit Amplitude	χ^2	Flux [$\mathrm{t\,day^{-1}}$]
2021-11-26	2 Plume A	200 m	11.8	501	2.33×10^6	2.07×10^4	$4.59 \pm 0.46 \times 10^3$
2021-11-27	6 Plume A	100 m	12.2	616	1.40×10^7	4.25×10^5	$2.85 \pm 0.28 \times 10^4$
2021-11-27	7 Plume B†	100 to 250 m	12.2	613	4.64×10^6	1.96×10^6	$9.44 \pm 0.94 \times 10^3$
2021-11-27	8 Plume A	300 m	12.2	577	3.18×10^6	2.77×10^5	$6.46 \pm 0.65 \times 10^3$
2021-11-28	9 Plume B†*	300 m	11.3	963	6.50×10^7	1.81×10^7	$1.22 \pm 0.12 \times 10^5$

3.1 Plume Transect Wind Measurements and CO_2 fluxes

The calculated CO_2 flux for the 5 relevant transects with the corresponding wind speeds are shown in Table 1 for transects across plume A and B. The wind speed measured by UAS drift method was $10.7\ \mathrm{ms^{-1}}$. ERA5 modeled wind speeds yielded results ranging from 10.0 to $12.2\ \mathrm{ms^{-1}}$ with an average of $11.0\ \mathrm{ms^{-1}}$.

3.2 Carbon isotopes of plume CO_2

The CO_2 concentrations and $\delta^{13}C$ values of plume gas samples are given in Table 2. Samples collected from the ground at the UNM Multi-GAS site show background CO_2 concentrations 416 to 471 ppm CO_2 with $\delta^{13}C$ values of -8‰ (relative to Peedee belemnite) which is close to that of air. The sample collected by UAS has a CO_2 concentration distinctly elevated from air of 671 ppm and a heavier $\delta^{13}C$ value of -4.44 ‰. Samples collected from the ground closer to the vent have even higher CO_2 concentrations from 1030 to 4459 ppm with $\delta^{13}C$ values from -2.40 to -1.47 ‰.

3.3 Multi-GAS measurements of plume

The Multi-GAS CO_2/SO_2 ratios during the period from November 21 to November 25, 2021 range from 5 to 26 and are shown in Table 2. These values are consistent with those reported by (Albertos et al., 2022) and (Burton et al., 2023). We use the range of reported SO_2 fluxes (mean of $10^4\ \mathrm{t\,day^{-1}}$ over the duration of the active eruption (Albertos et al., 2022)) in combination

Table 2. Measured CO_2 concentrations and $\delta^{13}C$ from ground and UAS.

Date	CO_2 [ppm]	$\delta^{13}C$ VPDB ‰	Collection method/site
2021-11-21	435	-7.46	Ground
2021-11-21	472	-8.34	Ground
2021-11-21	437	-7.65	Ground
2021-11-21	416	-8.00	Ground
2021-11-28	671	-4.44	UAS
2021-11-30	1030	-3.65	Ground
2021-11-30	2998	-2.12	Ground
2021-11-30	2863	-2.15	Ground
2021-12-01	4459	-2.03	Ground
2021-12-01	2722	-1.47	Ground
2021-12-01	1326	-2.40	Ground

Table 3. Multi-GAS measurements, SO_2 flux and computed CO_2 flux .

Date	Average CO_2/SO_2 (molar)	SO_2 flux (t/day)	CO_2 t/day
2021-11-21	26 ± 15	$2 \pm 1 \times 10^4$	$3.6 \pm 1.8 \times 10^5$
2021-11-22	10 ± 2	$2 \pm 1 \times 10^4$	$1.4 \pm 0.7 \times 10^5$
2021-11-23	5 ± 2	$2 \pm 1 \times 10^4$	$7.3 \pm 3.7 \times 10^4$
2021-11-24	7 ± 2	$2 \pm 1 \times 10^4$	$9.5 \pm 4.8 \times 10^4$
2021-11-25	16 ± 2	$2 \pm 1 \times 10^4$	$2.3 \pm 1.1 \times 10^5$

with the range of our Multi-GAS CO_2/SO_2 ratios to obtain CO_2 fluxes ranging from 7.3×10^4 to $3.6 \times 10^5 \, \mathrm{t} \, CO_2 \, \mathrm{day}^{-1}$ for this period (Table 3).

4   Discussion

This work highlights our efforts collecting and analysing CO_2 gasses during the Tajogaite volcanic eruption. Through this work, we demonstrated the efficacy of using a UAS to study the CO_2 plumes associated with an in-process eruption.

4.1 CO_2 Emissions

Our UAS-based CO_2 emission estimation technique yields CO_2 fluxes using direct measurement with a single type of instrument. This simplifies the estimation of CO_2 flux. However, in-situ measurement during an active eruption is challenging. The most serious difficulty we encountered was obtaining complete transects across the plume or plumes. In several of our transects, especially for the more distant Plume B, we were not successful in flying the UAS far enough to get to background CO_2 on the
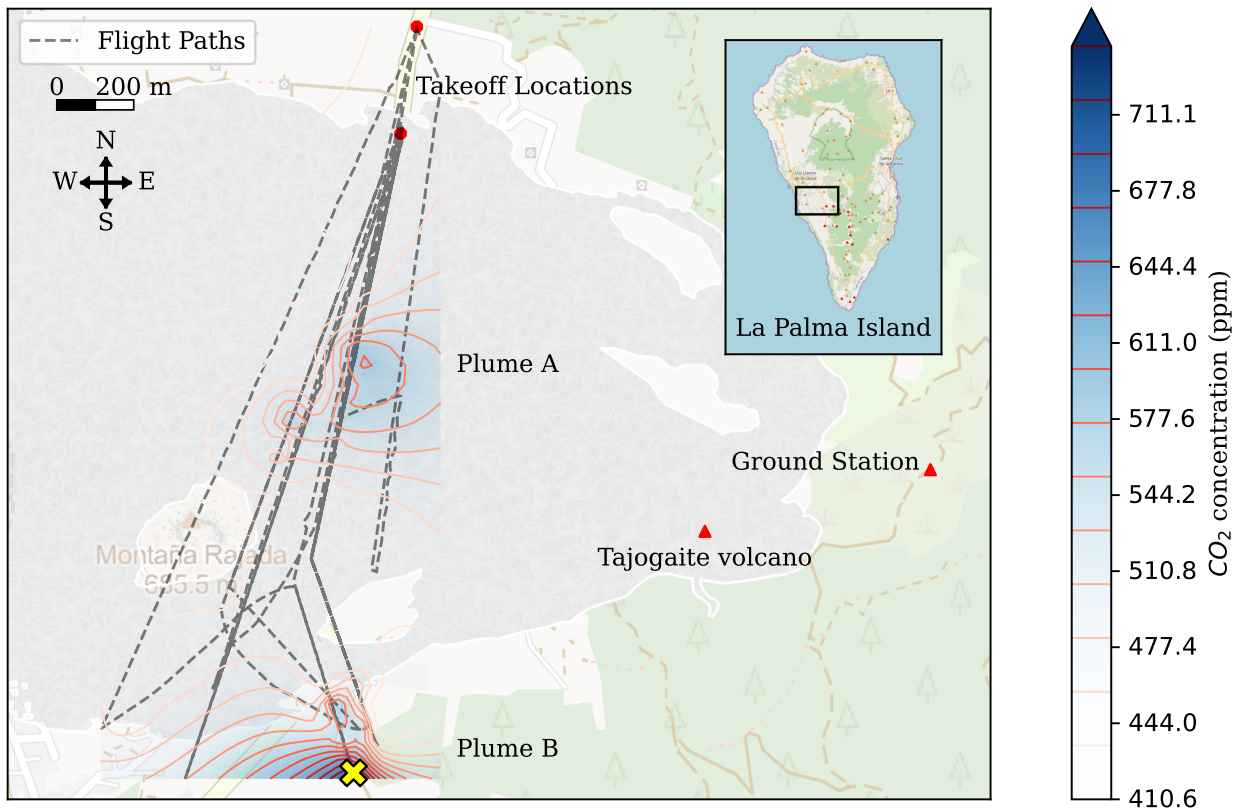
Figure 2. Top-down perspective map of all transect flight paths. Flights occurred over a four-day period during the 2021 eruption. This map includes a horizontal cross-section Kriging plot of the CO_2 concentration highlighted as the distinct Plumes A and B. The sample collection location is indicated by the yellow $\times$. Insert shows the location of Tajogaite Volcano on La Palma Island.

far side of the plume. Gas plumes change shape and direction on relatively short-time scales as the wind shifts. While ideally, we would like to perform several flights at various altitudes through a plume in order to obtain a complete CO_2 concentration map of the plume, this is challenging for wide or distant plumes because of limited UAS flight times and the need to know the plume's location and extent a priori. To address this challenge we assume a Gaussian plume and fit a Gaussian curve to our data. We then rotate the Gaussian fit to obtain a 2D concentration slice which is multiplied with estimated wind speed to yield the flux. This approach produces the most accurate results if we transect the plume through its widest part. However, identifying the widest part and then transecting the plume before the plume changes will require teams of collaborating UASs. A good fit of the data by the Gaussian model is given by a low χ^2 value. For instance, transect 2 was fit with a χ^2 value of 2.07×10^4, two orders of magnitude lower than the Gaussian fit amplitude of 2.33×10^6. The model fit represented by this low χ^2 value is depicted in Figure 4.
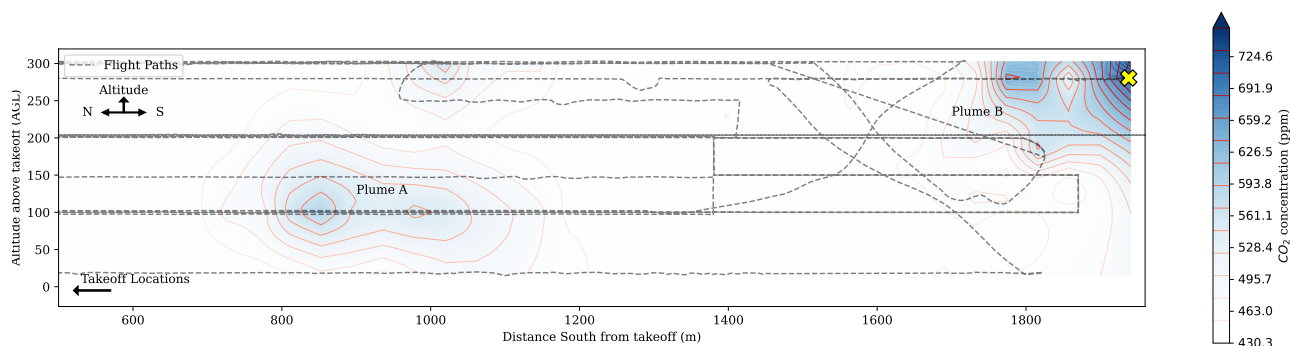
Figure 3. Lateral perspective kriging map of all transects plotted in Figure 2. The plot indicates two separate plumes in the vertical cross-section labeled Plume A and Plume B. The sample collection location is indicated by the yellow $\times$.

Uncertainty is introduced by the assumptions made by the model. With just one horizontal transect, we assume the vertical Gaussian standard deviation is identical to the horizontal standard deviation of the plume. Both dimension standard deviations are linearly correlated to the flux calculation, meaning that a 50% error in the vertical standard deviation will affect the flux estimate by a factor of 50%. Our estimate is that the vertical standard deviation is likely close to the horizontal standard deviation, but the difference is impossible to determine. Additionally, we assume that the horizontal transect samples the plume at the altitude where the plume is widest. If the transect is not through the largest cross-section, the flux calculation may be a lower bound. Wind velocity was measured during one of the transects, but weather is notoriously unpredictable. This represents another source of uncertainty in the model which has a linear effect on the flux measurement. We use our wind estimates during the time of each flux calculation. This wind speed variation gives an error range of $\pm10\%$. Additional sources of uncertainty such as sensor or location error are negligible in comparison to the aforementioned uncertainty. Therefore our estimated error range is $\pm10\%$.

Our data show that for Plume A, transect 6 (Figure 3) represents the widest plume and results in the highest CO_2 flux value of $2.85 \times 10^4 \, \text{t day}^{-1}$, an order of magnitude higher than the other two Plume A transects. This transect was flown at the lowest altitude (100 m) of the three, implying that the other two transects only captured the upper parts of the plume. Comparison with CO_2 fluxes obtained by combining SO_2 fluxes with CO_2 to SO_2 ratios measured 1 km from the vent gives fluxes ranging from 7.3×10^4 to $3.6 \times 10^5 \, \text{t} \, CO_2 \, \text{day}^{-1}$ (Table 3). Therefore our highest flux measurement is consistent with the lowest estimate using the combined method. While comparing these two approaches is helpful, our experiment was not designed to make a direct comparison. The discrepancy could be due to a significantly varying CO_2 emission rate during eruptions, an overestimate of the SO_2 flux, or the lack of validity of the 2D Gaussian extrapolation approach. Our estimates are consistent with the October 2021 high emissions presented by Bruton et al., 2023 who report fluxes of 3.36×10^4 to $4.19 \times 10^4 \, \text{t} \, CO_2 \, \text{day}^{-1}$ (389 to 486 kg/s) for the smaller, non-ashy plume that we measured. More work needs to be performed in the future to better assess sources
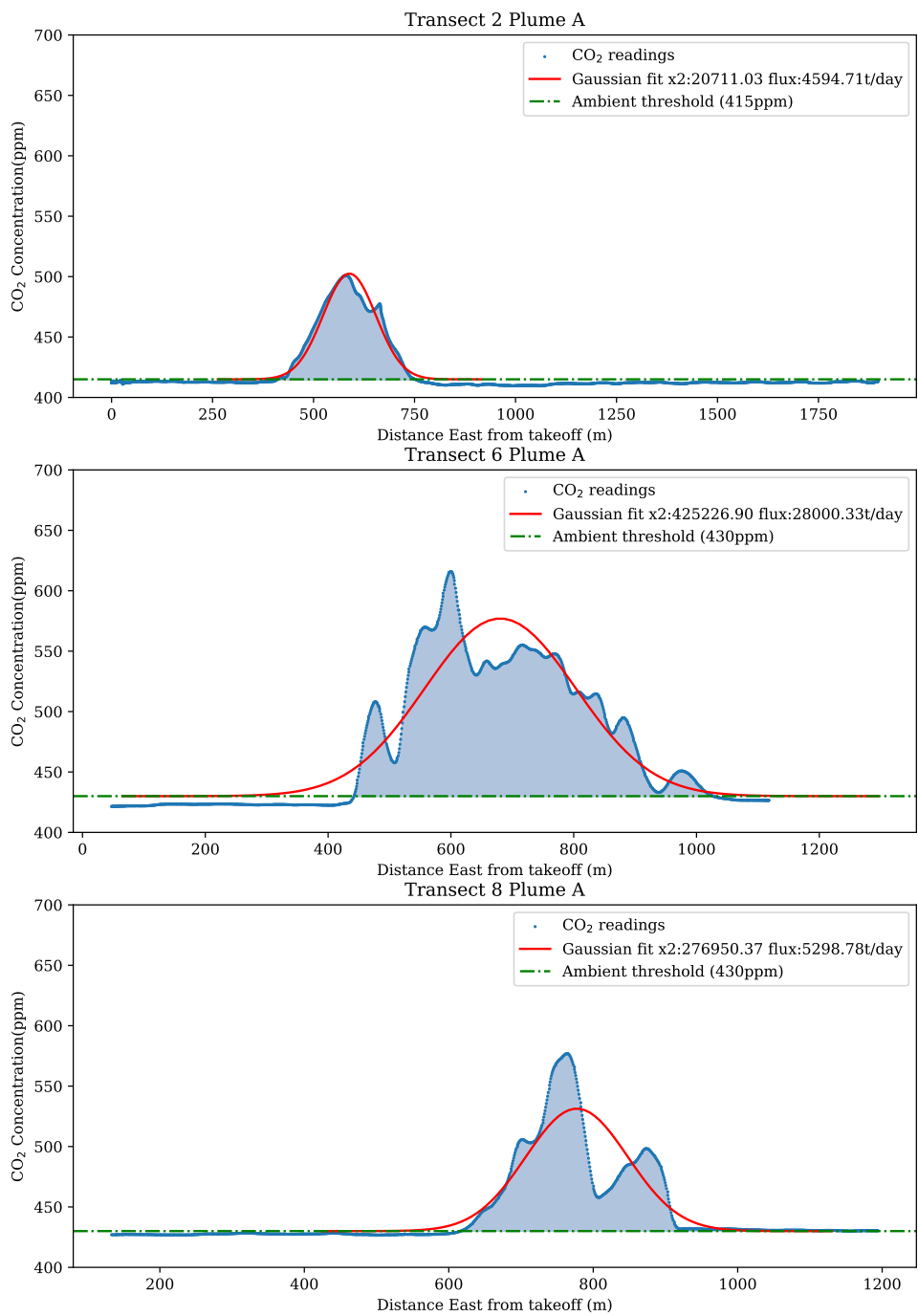
Figure 4. Three plots of encounters with plume A with the closest Gaussian model fit. CO_2 concentration (blue) over the encountered plume as a function of distance from takeoff location.
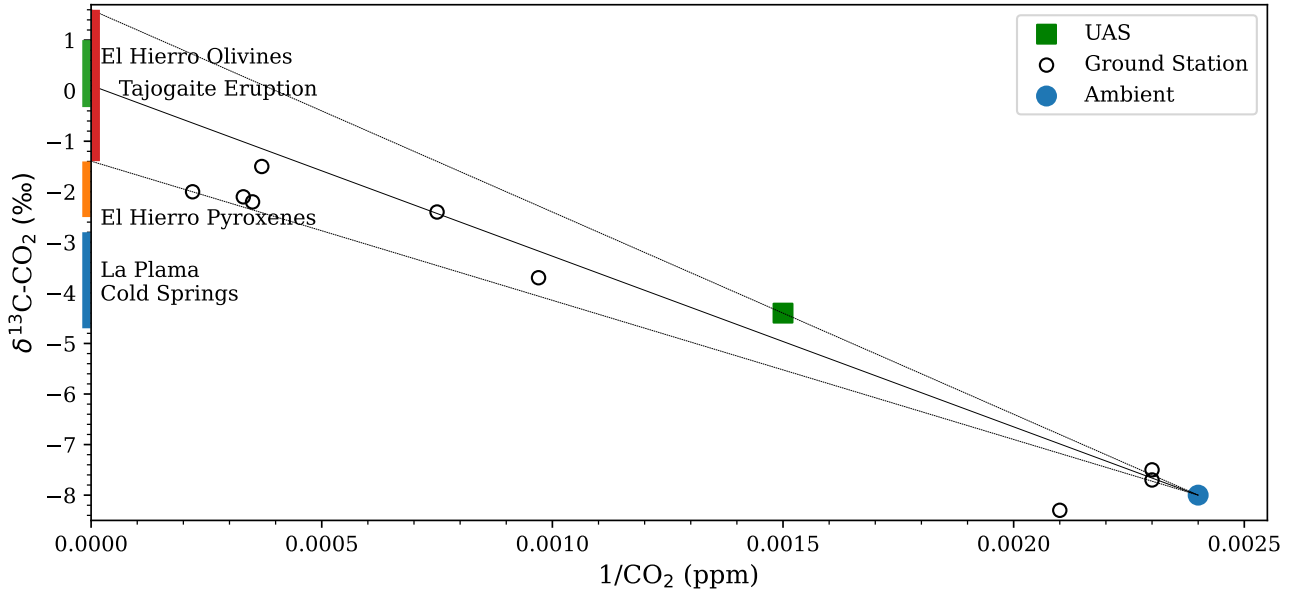
Figure 5. Keeling plot showing standard air, samples collected on the ground, and with the UAS. Linear extrapolation indicates a volcanic $\delta^{13}C - CO_2$ value of -1.40 to 1.60 ‰. Also shown are data from olivines and pyroxenes collected at the El Hierro Volcano (Sandoval-Velasquez et al., 2021) and the composition of cold CO_2-rich gas discharges on La Palma Island (Padrón et al., 2015).

of discrepancies with new and coordinated measurements at passively degassing and erupting volcanoes. However, even with such discrepancies, it is clear that the Tajogaite eruption in November 2021 produced a CO_2 flux up to $2 \times 10^4 \, \text{t day}^{-1}$ or even $5 \times 10^5 \, \text{t day}^{-1}$. Even the $5 \times 10^5 \, \text{t day}^{-1}$ would be only 0.4% of the daily CO_2 emitted by the burning of fossil fuels (Conlen, 2021).

4.2 Carbon Isotopes

The carbon isotope data obtained from the UAS-captured samples and the samples collected from the ground are generally consistent and show mixing of air-derived CO_2 with a deep magmatic source. Figure 5 shows that all plume samples collected from the ground define a set of mixing lines in $\delta^{13}C$ versus CO_2^{-1} space, i.e. in a Keeling plot (Keeling, 1958) that allows for the extrapolation of the $\delta^{13}C$ value of the pure CO_2 being emitted from the volcanic vent. The sample collected by UAV lies slightly above this set of mixing lines and extrapolates to somewhat heavier $\delta^{13}C$. The resulting volcanic $\delta^{13}C$ values taking into account all samples lies between -1.5 and +1.5 ‰. Despite these uncertainties, these values overlap with $\delta^{13}C$ data obtained from mantle xenoliths erupted at the nearby El Hierro Volcano (Sandoval-Velasquez et al., 2021). Extrapolation of all these data results in a $\delta^{13}C$ value of 0.1 ± 1.5‰. Notably the carbon isotope values are significantly heavier than those measured in cold CO_2-rich gas discharges from springs on La Palma (Padrón et al., 2015) and within the range of values measured in

olivines and pyroxenes of xenoliths from El Hierro Island (Sandoval-Velasquez et al., 2021). These authors suggested that the heavy values of the xenoliths are related to recycling of crustal carbon, likely derived from carbonates into the mantle source of the Canary Islands hot spot. Our data suggests that the magmatic system that is driving the Tajogaite eruption taps into this deep CO_2, rather than remobilizing CO_2 that feeds the cold degassing springs on the island. Sandoval-Velasquez et al. (2024) report $\delta^{13}C$ values measured in olivines, clinopyroxenes and orthopyroxenes from lava flows erupted in 2021. Their data is consistent with our extrapolated heavy $\delta^{13}C$ values. For olivines, representing the earliest crystallization phase, their values range from 0 to 1‰. Values are somewhat lighter for orthopyroxenes and clinopyroxenes. Using all data, their estimated mantle endmember is -1.5‰. Our data extrapolate to -1.4 to +1.6‰. Given the difference in sample medium, i.e. phenocrysts versus gas plume, the results are remarkably consistent. More work at erupting volcanoes is needed to better constrain the sources of magmatic CO_2 emitted during heightened activity of volcanic systems.

5 Conclusion

The use of UAS is revolutionizing volcano science by enabling the collection of data that previously required extensive, costly, and hazardous aerial surveys using piloted fixed-wing aircraft or helicopters. Especially in the field of volcanic gases, recent UAS-based campaigns showed the value of utilizing UAS to make gas flux and gas composition measurements and also collect plume samples for subsequent chemical and isotopic analyses (Liu et al., 2020; Galle et al., 2021). Our work during the explosive and hazardous eruption of the Tajogaite Volcano shows that CO_2 emission measurements and plume gas samples can be collected even during these heightened periods of volcanic activity. We demonstrate that a UAS capable of automated sampling can be guided by the expert knowledge of scientists in the field to collect valuable data that would be impossible with robots or scientists alone. The collected data provide key insights into the volcano's state and the course of an eruption. Future work is needed to increase UAS autonomy in choosing flight paths to more completely capture data from dynamic plumes, but, as we have demonstrated, the present approach works for volcano monitoring during eruptions and can provide much-needed information about eruptive gas emissions.

Code and data availability. Additional data and plot generation code is available at https://github.com/BCLab-UNM/lapalma-expedition/tree/2021_tajogaite_eruption. UAS code available at https://github.com/BCLab-UNM/dragonfly-dashboard https://github.com/BCLab-UNM/dragonfly-controller.
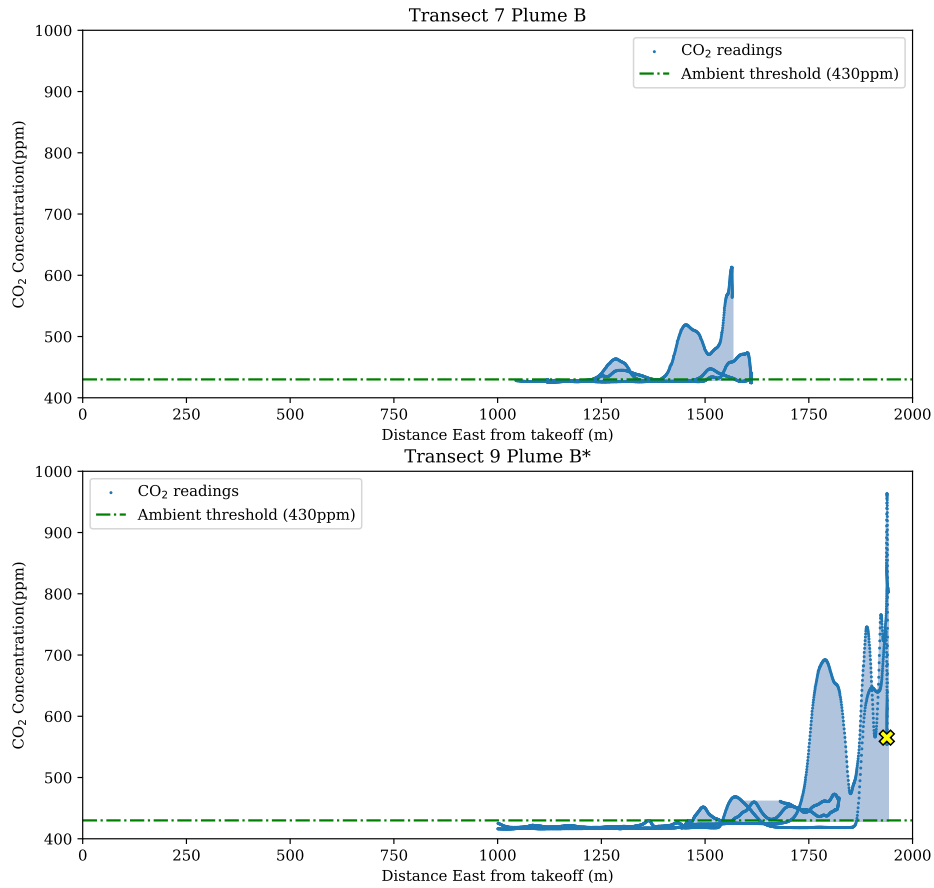
Figure A1. Encounters with plume B were not as well-fit as plume A encounters. These plots show the CO_2 readings collected during the two highest plume model fit. As with Figure 4, CO_2 concentration (blue) over the encountered plume as a function of distance from takeoff location. The sample collection location is indicated by the yellow $\times$.

Author contributions. Author contributions: JE, GMF, SN, and TF (UNM VolCAN team) performed UAS fieldwork for this paper. JE, NP, PHP, EPG (INVOLCAN team) and TF conducted the ground fieldwork. JE developed UAS software and hardware supervised by GMF and MEM. SN designed the sample collection device. JE, NP, PHP, EPG performed data analysis. TF performed isotope and gas analysis. JE, TF, GMF, SN, and MEM wrote the manuscript.

Competing interests. The authors declare that they have no competing interests. The authors give consent for publication. All data needed to evaluate the conclusions in the paper are present in the paper and/or the Supplementary Materials.

Acknowledgements. JE support provided by the Department of Energy's Kansas City National Security Campus, operated by Honeywell Federal Manufacturing & Technologies, LLC under contract number DE-NA0002839. GMF, SN, TF, RF, and MM support provided by the VolCAN project under National Science Foundation grant 2024520. Support was also provided by a Google CSR award. This study received funding from Google and Honeywell Federal Manufacturing & Technologies, LLC. VOLRISKMAC II (MAC2/3.5b/328) financed by the Program INTERREG V A Spain-Portugal MAC 2014-2020 of the European Commission. Thanks to Samantha Wolf for help calculating the flux.

References

Acocella, V., Di Lorenzo, R., Newhall, C., and Scandone, R.: An overview of recent (1988 to 2014) caldera unrest: Knowledge and perspectives, https://doi.org/10.1002/2015RG000492, 2015.

255   Albert, H., Costa, F., and Martí, J.: Years to weeks of seismic unrest and magmatic intrusions precede monogenetic eruptions, Geology, 44, https://doi.org/10.1130/G37239.1, 2016.

Albertos, V. T., Recio, G., Alonso, M., Amonte, C., Rodríguez, F., Rodríguez, C., Pitti, L., Leal, V., Cervigón, G., González, J., Przeor, M., Santana-León, J. M., Barrancos, J., Hernández, P. A., Padilla, G. D., Melián, G. V., Padrón, E., Asensio-Ramos, M., and Pérez, N. M.: Sulphur dioxide (SO2) emissions by means of miniDOAS measurements during the 2021 eruption of Cumbre Vieja volcano, La Palma,
260   Canary Islands, EGU22, https://doi.org/10.5194/EGUSPHERE-EGU22-5603, 2022.

Arrhenius, S.: On the Influence of Carbonic Acid in the Air upon the Temperature of the Ground, Philos. Mag, 41, 237, 1896.

Burton, M., Aiuppa, A., Allard, P., Asensio-Ramos, M., Cofrades, A. P., La Spina, A., Nicholson, E. J., Zanon, V., Barrancos, J., Bitetto, M., Hartley, M., Romero, J. E., Waters, E., Stewart, A., Hernández, P. A., Lages, J. P., Padrón, E., Wood, K., Esse, B., Hayer, C., Cyrzan, K., Rose-Koga, E. F., Schiavi, F., D'Auria, L., and Pérez, N. M.: Exceptional eruptive CO2 emissions from intra-plate alkaline magmatism in
265   the Canary volcanic archipelago, Communications Earth & Environment 2023 4:1, 4, 1–10, https://doi.org/10.1038/s43247-023-01103-x, 2023.

Burton, M. R., Sawyer, G. M., and Granieri, D.: Deep Carbon Emissions from Volcanoes, Reviews in Mineralogy and Geochemistry, 75, 323–354, https://doi.org/10.2138/RMG.2013.75.11, 2013.

Carracedo, J. C., Day, S., Guillou, H., Rodríguez Badiola, E., Canas, J. A., and Pérez Torrado, F. J.: Hotspot volcanism close to a passive
270   continental margin: the Canary Islands, Geological Magazine, 135, 591–604, https://doi.org/10.1017/S0016756898001447, 1998.

Carracedo, J. C., Badiola, E. R., Guillou, H., De La Nuez, J., and Pérez Torrado, F. J.: Geology and volcanology of la Palma and el Hierro, western Canaries, Estudios Geologicos, 57, 2001.

Castro, J. M. and Feisel, Y.: Eruption of ultralow-viscosity basanite magma at Cumbre Vieja, La Palma, Canary Islands, Nature Communications 2022 13:1, 13, 1–12, https://doi.org/10.1038/s41467-022-30905-4, 2022.

275   Conlen, M.: How Much Carbon Dioxide Are We Emitting? – Climate Change: Vital Signs of the Planet, https://climate.nasa.gov/news/3020/how-much-carbon-dioxide-are-we-emitting/, 2021.

Day, S. J., Carracedo, J. C., Guillou, H., and Gravestock, P.: Recent structural evolution of the Cumbre Vieja volcano, La Palma, Canary Islands: Volcanic rift zone reconfiguration as a precursor to volcano flank instability?, Journal of Volcanology and Geothermal Research, 94, https://doi.org/10.1016/S0377-0273(99)00101-8, 1999.

280   De Luca, C., Valerio, E., Giudicepietro, F., Macedonio, G., Casu, F., and Lanari, R.: Pre-and Co-Eruptive Analysis of the September 2021 Eruption at Cumbre Vieja Volcano (La Palma, Canary Islands) Through DInSAR Measurements and Analytical Modeling, Geophysical Research Letters, 49, e2021GL097 293, 2022.

Ericksen, J., Fricke, G. M., Nowicki, S., Fischer, T. P., Hayes, J. C., Rosenberger, K., Wolf, S. R., Fierro, R., and Moses, M. E.: Aerial Survey Robotics in Extreme Environments: Mapping Volcanic CO2 Emissions With Flocking UAVs, Frontiers in Control Engineering, 0,
285   7, https://doi.org/10.3389/FCTEG.2022.836720, 2022.

Fernández, J., Escayo, J., Hu, Z., Camacho, A. G., Samsonov, S. V., Prieto, J. F., Tiampo, K. F., Palano, M., Mallorquí, J. J., and Ancochea, E.: Detection of volcanic unrest onset in La Palma, Canary Islands, evolution and implications, Scientific Reports, 11, https://doi.org/10.1038/s41598-021-82292-3, 2021.

Fischer, T. P. and Aiuppa, A.: AGU Centennial Grand Challenge: Volcanoes and Deep Carbon Global CO2 Emissions From Subaerial Vol-
canism—Recent Progress and Future Challenges, Geochemistry, Geophysics, Geosystems, 21, https://doi.org/10.1029/2019GC008690,
2020.

Fischer, T. P. and Lopez, T. M.: First airborne samples of a volcanic plume for δ13C of CO2 determinations, Geophysical Research Letters,
43, 3272–3279, https://doi.org/10.1002/2016GL068499, 2016.

Fischer, T. P., Arellano, S., Carn, S., Aiuppa, A., Galle, B., Allard, P., Lopez, T., Shinohara, H., Kelly, P., Werner, C., Cardellini,
C., and Chiodini, G.: The emissions of CO2 and other volatiles from the world's subaerial volcanoes, Scientific Reports, 9,
https://doi.org/10.1038/s41598-019-54682-1, 2019.

Galle, B., Arellano, S., Bobrowski, N., Conde, V., Fischer, T. P., Gerdes, G., Gutmann, A., Hoffmann, T., Itikarai, I., Krejci, T., Liu, E. J.,
Mulina, K., Nowicki, S., Richardson, T., Rüdiger, J., Wood, K., and Xu, J.: A multi-purpose, multi-rotor drone system for long-range and
high-altitude volcanic gas plume measurements, Atmospheric Measurement Techniques, 14, https://doi.org/10.5194/amt-14-4255-2021,
2021.

Gerlach, T. M., Delgado, H., McGee, K. A., Doukas, M. P., Venegas, J. J., and Cárdenas, L.: Application of the LI-COR CO2 analyzer to
volcanic plumes: A case study, volcán Popocatépetl, Mexico, June 7 and 10, 1995, Journal of Geophysical Research: Solid Earth, 102,
8005–8019, https://doi.org/10.1029/96JB03887, 1997.

Giggenbach, W. F.: Chemical Composition of Volcanic Gases, Monitoring and Mitigation of Volcano Hazards, pp. 221–256, https://link.
springer.com/chapter/10.1007/978-3-642-80087-0_7, 1996.

Ilanko, T., Fischer, T. P., Kyle, P., Curtis, A., Lee, H., and Sano, Y.: Modification of fumarolic gases by the ice-covered edifice of Erebus vol-
cano, Antarctica, Journal of Volcanology and Geothermal Research, 381, 119–139, https://doi.org/10.1016/J.JVOLGEORES.2019.05.017,
2019.

Instituto Geográfico Nacional: Noticias e informe mensual de vigilancia volcánica, https://www.ign.es/web/resources/volcanologia/html/
CA_noticias.html, 2022.

Johnson, M. S., Schwandner, F. M., Potter, C. S., Nguyen, H. M., Bell, E., Nelson, R. R., Philip, S., and O'Dell, C. W.: Carbon Dioxide
Emissions During the 2018 Kilauea Volcano Eruption Estimated Using OCO-2 Satellite Retrievals, Geophysical Research Letters, 47,
e2020GL090 507, https://doi.org/10.1029/2020GL090507, 2020.

Keeling, C. D.: The concentration and isotopic abundances of atmospheric carbon dioxide in rural areas, Geochimica et Cosmochimica Acta,
13, https://doi.org/10.1016/0016-7037(58)90033-4, 1958.

León, J. M. S. d., Melián, G. V., Rodríguez, C., Cervigón-Tomico, G., Ortega, V., Dorth, D. M. v., Cabrera-Pérez, I., Cordero, M., Przeor, M.,
Silva, R. F. F., Matos, S. B. d., Baldoni, E., Ramalho, M. M. P., Viveiros, F., Calvo, D., and Pérez, N. M.: Long-term variations of diffuse
CO2 at Cumbre Vieja volcano, La Palma, Canary Islands, EGU22, https://doi.org/10.5194/EGUSPHERE-EGU22-8773, 2022.

Liu, E. J., Aiuppa, A., Alan, A., Arellano, S., Bitetto, M., Bobrowski, N., Carn, S., Clarke, R., Corrales, E., De Moor, J. M., Diaz, J. A.,
Edmonds, M., Fischer, T. P., Freer, J., Fricke, G. M., Galle, B., Gerdes, G., Giudice, G., Gutmann, A., Hayer, C., Itikarai, I., Jones, J.,
Mason, E., McCormick Kilbride, B. T., Mulina, K., Nowicki, S., Rahilly, K., Richardson, T., Rüdiger, J., Schipper, C. I., Watson, I. M.,
and Wood, K.: Aerial strategies advance volcanic gas measurements at inaccessible, strongly degassing volcanoes, Science Advances, 6,
https://doi.org/10.1126/sciadv.abb9103, 2020.

Office of Science, US DOE: FLUXNET, http://fluxnet.org, 2023.

325   Padrón, E., Pérez, N. M., Rodríguez, F., Melián, G., Hernández, P. A., Sumino, H., Padilla, G., Barrancos, J., Dionis, S., Notsu, K., and Calvo, D.: Dynamics of diffuse carbon dioxide emissions from Cumbre Vieja volcano, La Palma, Canary Islands, Bulletin of Volcanology, 77, https://doi.org/10.1007/s00445-015-0914-2, 2015.

Pérez, N. M., Hernández, P. A., Melián, G. V., Padrón, E., Asensio-Ramos, M., Barrancos, J., Padilla, G. D., Rodríguez, F., D'Auria, L., Amonte, C., Alonso, M., Martín-Lorenzo, A., Calvo, D., Rodríguez, C., Hernández, W., Coldwell, B., and Pankhurst, M. J.: The 2021

330   Cumbre Vieja eruption: an overview of the geochemical monitoring program, EGU22, https://doi.org/10.5194/EGUSPHERE-EGU22-12491, 2022.

Rodríguez-Pérez, C., Barrancos, J., Hernández, P. A., Pérez, N. M., Padrón, E., Melián, G. V., Rodríguez, F., Asensio-Ramos, M., and Padilla, G. D.: Continuous monitoring of diffuse CO2 emission from Cumbre Vieja volcano: early evidences of magmatic CO2 surface arrival, Tech. rep., Copernicus Meetings, 2022.

335   Rüdiger, J., Tirpitz, J. L., Maarten De Moor, J., Bobrowski, N., Gutmann, A., Liuzzo, M., Ibarra, M., and Hoffmann, T.: Implementation of electrochemical, optical and denuder-based sensors and sampling techniques on UAV for volcanic gas measurements: Examples from Masaya, Turrialba and Stromboli volcanoes, Atmospheric Measurement Techniques, 11, https://doi.org/10.5194/amt-11-2441-2018, 2018.

Sandoval-Velasquez, A., Rizzo, A. L., Aiuppa, A., Remigi, S., Padrón, E., Pérez, N. M., and Frezzotti, M. L.: Recycled crustal carbon in the depleted mantle source of El Hierro volcano, Canary Islands, Lithos, 400-401, https://doi.org/10.1016/j.lithos.2021.106414, 2021.

340   Sandoval-Velasquez, A., Casetta, F., Ntaflos, T., Aiuppa, A., Coltorti, M., Frezzotti, M. L., Alonso, M., Padrón, E., Pankhurst, M., Pérez, N. M., and Rizzo, A. L.: 2021 Tajogaite eruption records infiltration of crustal fluids within the upper mantle beneath La Palma, Canary Islands, Frontiers in Earth Science, 12, 1303 872, https://doi.org/10.3389/FEART.2024.1303872/BIBTEX, 2024.

Schmincke, H. U.: Volcanic and chemical evolution of the Canary Islands, Geology of the northwest African continental margin, pp. 273–306, https://doi.org/10.1007/978-3-642-68409-8_12/COVER, 1982.

345   Schwandner, F. M., Gunson, M. R., Miller, C. E., Carn, S. A., Eldering, A., Krings, T., Verhulst, K. R., Schimel, D. S., Nguyen, H. M., Crisp, D., O'Dell, C. W., Osterman, G. B., Iraci, L. T., and Podolske, J. R.: Spaceborne detection of localized carbon dioxide sources, Science, 358, https://doi.org/10.1126/science.aam5782, 2017.

Stix, J., de Moor, J. M., Rüdiger, J., Alan, A., Corrales, E., D'Arcy, F., Diaz, J. A., and Liotta, M.: Using Drones and Miniaturized Instrumentation to Study Degassing at Turrialba and Masaya Volcanoes, Central America, Journal of Geophysical Research: Solid Earth, 123,

350   6501–6520, https://doi.org/10.1029/2018JB015655, 2018.

Ward, S. N. and Day, S.: Cumbre Vieja Volcano-Potential collapse and tsunami at La Palma, Canary Islands, Geophysical Research Letters, 28, https://doi.org/10.1029/2001GL013110, 2001.

Werner, C., Kelly, P. J., Doukas, M., Lopez, T., Pfeffer, M., McGimsey, R., and Neal, C.: Degassing of CO2, SO2, and H2S associated with the 2009 eruption of Redoubt Volcano, Alaska, Journal of Volcanology and Geothermal Research, 259, 270–284,

355   https://doi.org/10.1016/J.JVOLGEORES.2012.04.012, 2013.

Xi, X., Johnson, M. S., Jeong, S., Fladeland, M., Pieri, D., Diaz, J. A., and Bland, G. L.: Constraining the sulfur dioxide degassing flux from Turrialba volcano, Costa Rica using unmanned aerial system measurements, Journal of Volcanology and Geothermal Research, 325, 110–118, https://doi.org/10.1016/J.JVOLGEORES.2016.06.023, 2016.